

The Irradiation Resistance of Zr-1.8Nb Alloy under the 140 MeV C⁴⁺ Irradiation

著者	Kano S., Yang H., Zhao Z., McGrady J.P., Itoh M., Tanaka K.S., Abe H.
journal or publication title	CYRIC annual report
volume	2016-2017
page range	66-66
year	2017
URL	http://hdl.handle.net/10097/00128062

III. 2. The Irradiation Resistance of Zr-1.8Nb Alloy under the 140 MeV-C⁴⁺ Irradiation

Kano S.¹, Yang H.¹, Zhao Z.¹, McGrady J.P.¹, Itoh M.², Tanaka K.S.², and Abe H.¹

¹*Department of Nuclear Engineering, The University of Tokyo*

²*Cyclotron and Radioisotope Center, Tohoku University*

The material examined in the present study was a Zr-1.8Nb (wt.%) alloy recently developed as the fuel cladding tubes of pressurized water reactors. Such kind of Zr-based alloys are widely reported to exhibit remarkable hardening/strengthening due to the irradiation, typically ~100 MPa increase in the yield strength (YS) at room temperature^{1,2}. The irradiation defects in Zr-based alloys (i.e. dislocation loops) are divided into two groups: the <a>-type loop formed on the prismatic planes and the <c>-type loop on the basal plane. The <a>-type loop is either vacancy or interstitial nature; in both cases the Burgers vector (*b*) is $1/3 \langle 112\bar{0} \rangle$. This type of dislocation loop is produced with low doses less than $5 \times 10^{25} \text{ n/m}^2$ ³. The size is typically 5–20 nm and the number density is $10^{21} \text{--} 10^{22} / \text{m}^3$ primarily depending on the irradiation temperature. At high doses greater than $\sim 5 \times 10^{25} \text{ n/m}^2$ the <c>-type dislocation loops start to appear. They are mainly vacancy-type in nature and the Burgers vector is either $1/2 \langle 0001 \rangle$ or $1/6 \langle 202\bar{3} \rangle$ ⁴⁻⁶. The <c>-type loop is in many cases larger than the <a>-type loop in terms of size and lower in number density. The <c>-type dislocation loops are extensively believed to be closely related to performance degradations such as irradiation growth and the ductility loss induced by irradiation⁷⁻¹⁰. Therefore, the aim of the present study is to examine the irradiation resistance in the new developed Zr-1.8Nb alloy in terms of mechanical property change and irradiation defects evolution.

The tube shaped Zr-1.8 Nb (wt.%) alloy was used as the start materials. The tube was firstly cut in half, and the half piece was subsequently cold-rolled into a flat sheet. The thickness was reduced from 0.55 to 0.38 mm. The rolling direction was parallel to the axial direction of the tube. Finally, the cold-rolled sheets were annealed at 853 K for 24 h in vacuum ($< 5 \times 10^{-4} \text{ Pa}$) and followed by cooling, so as to recrystallize the Zr matrix.

The small size tensile specimens (gauge section: 5 mm in length and 1.2 mm in width)

were punched out from the cold-rolled and annealed sheets with the length direction being perpendicular to the rolling direction. Both sides of tensile specimens were mechanically grinded and finished with mechano-chemical polishing in a suspension of 0.05 μm silica particles. The final thickness of tensile specimens was 180 ± 5 μm .

140 MeV- C^{4+} ion beam was employed to irradiate the tensile specimens mounted on a sample stage equipped with a heating/cooling temperature-control system in the Cyclotron and Radioisotope Center, Tohoku University¹¹⁾. The temperature was continuously monitored and recorded by a thermocouple fixed in the vicinity of specimen throughout the irradiation. The irradiation temperature was carefully controlled at 573 ± 10 K. Displacement damage was determined from the fraction of vacancies calculated by Kinchin-Pease option in SRIM code¹²⁾, with the displacement threshold energies of 40 MeV for Zr. Penetration depth of the 140 MeV- C^{4+} in Zr is ~ 180 μm , comparable to the thickness of tensile specimens. In order to create spatially homogeneous irradiation defects, a variable energy degrader was used. It is a rotating wheel system consisting of a set of Al foils with the thickness ranging from 0 to 284 μm , which enables to produce the roughly homogeneous distribution of irradiation defects throughout the specimen thickness. The beam current density was 3.4×10^{-3} A/ m^2 , Tensile specimens with displacement damages of roughly 0.2, 1.7, 3.1 and 5.3 dpa (displacement per atoms) were achieved in the present study. Additionally, the amount of implantation C atoms was estimated as 230 at. ppm for 3.1 dpa specimen.

Tensile tests were carried out at room temperature and the strain rate was set to 10^{-3} /s with a high-accuracy laser displacement measurer. Microstructure characterization was performed using 200 keV transmission electron microscopes (TEM). The TEM specimen was lifted out from the unstrained tensile specimens via a focused ion beam (FIB) technique.

The stress-strain (σ - ϵ) curves for unirradiated and irradiated specimens are shown in Fig. 1. The total elongation of unirradiated specimen was 25%, which was decreased evidently due to irradiation. Note that the uniform elongation was nearly zero for the highly irradiated specimens (3.1 and 5.3 dpa); this is probably an indication of the occurrence of the dislocation channeling. Both the yield strength (YS) and ultimate tensile strength (UTS) drastically increased at low doses below 1 dpa, and increased moderately beyond that point. The YS for the 3.1 and 5.3 dpa specimens was 137% and 145% of that of unirradiated specimen, whereas the uniform/total elongation for the 3.1 and 5.3 dpa specimens was less than a half of unirradiated specimen. A comparison of these two indicates that the rate of embrittlement is fairly faster than the rate of strengthening.

In the analysis of irradiation defect clusters, observation of the <c>-type loops were

performed from a direction close to the $[11\bar{0}0]$ zone axis, where the $\langle c \rangle$ -type loops are in edge-on view parallel to the basal plane regardless of the Burgers vector. This aligned array of linear contrast was typical feature of $\langle c \rangle$ -type loops observed in irradiated Zr and its alloys^{7,13,14}. The diameter of the $\langle c \rangle$ -type loops was determined by the length of line segments visualized on TEM images. The diameter was in a range from 3 to 50 nm, and the mean diameter was 15.4 ± 7.4 nm. The number density of $\langle c \rangle$ -type loops was $6.5 \times 10^{20} / \text{m}^3$. Observation of the $\langle a \rangle$ -type loops was performed near the $[0001]$ zone axis. Seen from this direction, the $\langle a \rangle$ -type loops are in edge-on view parallel to the prismatic planes. The $\langle c \rangle$ -type loops are invisible in the case of $b=1/2 \langle 0001 \rangle$ but visible in the case of $b=1/6 \langle 202\bar{3} \rangle$; however, those visible $\langle c \rangle$ -type loops are distinguishable from the $\langle a \rangle$ -type loops by shape on the TEM image. The diameter of $\langle a \rangle$ -type loops was in a range from ~ 3 to 30 nm, and the mean diameter was 7.2 ± 3.6 nm. The number density of $\langle a \rangle$ -type loops was $1.2 \times 10^{21} / \text{m}^3$.

In conclusion, 140 MeV-C⁴⁺ irradiation at 573 K up to 5.3 dpa was successfully conducted on a Zr-1.8Nb alloy to evaluate its mechanical properties change. The yield strength and the total elongation of 3.1 dpa irradiated specimens were $>137\%$ and $<50\%$ of unirradiated specimen, indicating that the rate of embrittlement is fairly faster than the rate of strengthening. TEM observation on the 3.1 dpa specimen revealed that the size and number density of dislocation loops were 7.2 nm and $1.2 \times 10^{21} / \text{m}^3$ for the $\langle a \rangle$ -loops, 15.4 nm and $6.5 \times 10^{20} / \text{m}^3$ for the $\langle c \rangle$ -type loops, respectively.

This research was supported by JST Innovative Nuclear Research and Development Project.

References

- 1) Boyne A, Shen C, Najafabadi R, Wang Y, J. Nucl. Mater. **438** (2013) 209.
- 2) Byun T, Farrell K, J. Nucl. Mater. **326** (2004) 86.
- 3) Northwood D, Gilbert R, Bahen L, Kelly P, Blake R, Jostsons A, Madden P, Faulkner D, Bell W, Adamson R, J. Nucl. Mater. **79** (1979) 379.
- 4) Griffiths M, J. Nucl. Mater. **159** (1988) 190.
- 5) Yan C, Wang R, Wang Y, Wang X, Bai G, Nucl. Eng. Technol. **47** (2015) 323.
- 6) Jin H, Kim T, Ann. Nucl. Energy **75** (2015) 309.
- 7) Tournadre L, Onimus F, Béchade J, Gilbon D, Cloué J, Mardon J, Feaugas X, Toader O, Bachelet C, J. Nucl. Mater. **425** (2012) 76.
- 8) Woo O, Carpenter G, MacEwen S, J. Nucl. Mater. **87** (1979) 70.
- 9) Yamada S, Kameyama T, J. Nucl. Mater. **422** (2012) 167.
- 10) Hengstler-Eger R, Baldo P, Beck L, Dorner J, Ertl K, Hoffmann P, Hugenschmidt C, Kirk M, Petry W, Pikart P, Rempel A, J. Nucl. Mater. **423** (2012) 170.
- 11) Orihara H, Murakami T, Nucl. Instrum. Methods **188** (1981) 15.
- 12) Ziegler J, Manoyan J, Nucl. Instrum. Methods B **35** (1988) 215.
- 13) Yamada S, Kameyama T, J. Nucl. Mater. **422** (2012) 167.
- 14) Holt R, Gilbert R, J. Nucl. Mater. **137** (1986) 185.

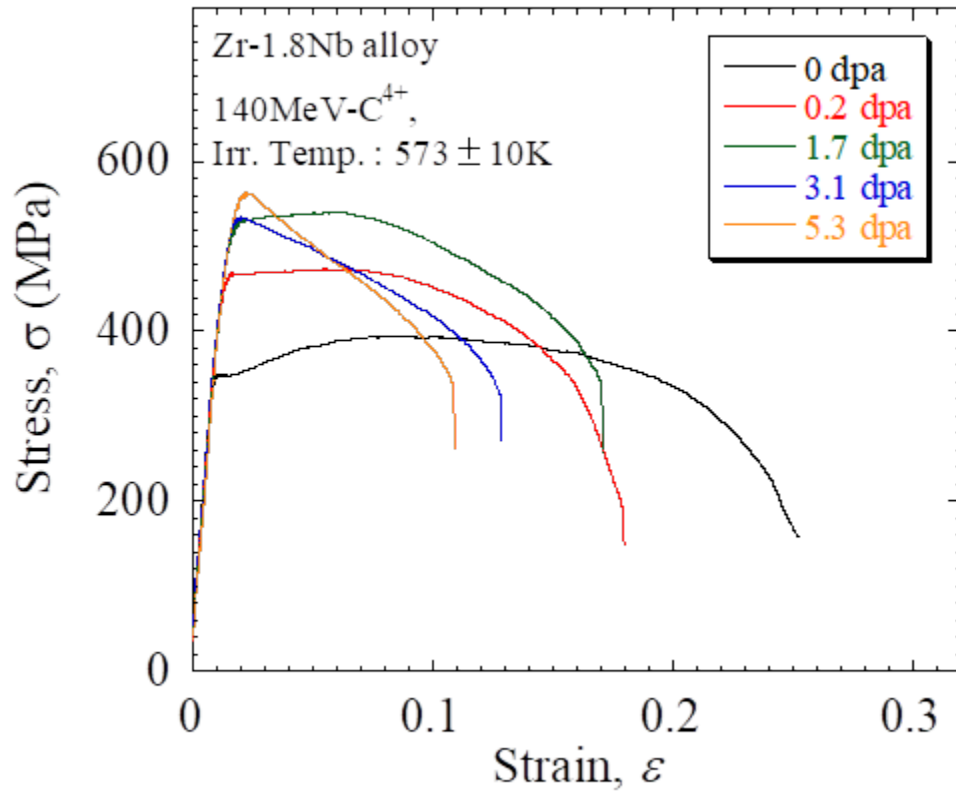


Figure 1. Stress-strain curves of irradiated and unirradiated Zr-1.8Nb alloy.